Experimental Study on Microscopic Performance of Underwater Concrete of a Sluice

Experimental Study on Microscopic Performance of Underwater Concrete of a Sluice

D D Li[1], D W Zhang[1]

[1]Nanjing Hydraulic Research Institute, Jiangsu Province, Nanjing ,210098, China.

Abstract. Zaohe Lock was built in the 1950s and has a long running time. The bottom plate, gate pier and apron (covered) parts of the gate were sampled this time, and concrete samples were tested for related performances at the same time, including microscopic pore structure, micromorphology and chemical composition. The results of this experiment will help us to understand the changes in physical and mechanical properties of underwater concrete and its durability changes, revealing the macro and microscopic performance evolution mechanisms of concrete materials, and providing technical reference for the durability design of related hydraulic structures.

1. Introduction

A sluice was built in 1951 and it had been in service for more than 60 years so far. It plays an important role in many aspects, such as flood discharge, irrigation, and regulation of water level for shipping. The sluice design flow is 500m3/s, and the check flow is 1000m3/s. The engineering grade is Ⅱ scale and the rank of major buildings is level 2. The flood control standards is 50-year-return period and the check flood is 100-year-return period. The gate is a reinforced concrete structure with a total of 7 holes with the net width of 9.2m, a net height of 4.0m with a total width of 71.25m. The floor elevation is 15.85m and it is divided into three sections. Piers and gate piers are divided, and there is a stilling pool and a lead wire cage block under the sluice, and a reinforced concrete impermeable retaining tank and a resistance skateboard at the upstream, and a dry block stone apron above. The gate is a curved steel gate equipped with a 2×7.5t hand and electric dual-purpose hoisting hoist. The upper reaches will have a working bridge, with an elevation of 25.00m and a width of 1.5m. In view of the long running time of the sluice, an experimental study was conducted on the internal microstructure of the underwater concrete to reveal the microscopic performance evolution mechanism of concrete materials, which could provide theoretical basis and technical support for further improvements to the design theory of hydraulic concrete structures and the safe operation level of hydraulic structures.

2. Formatting the title, authors and affiliations

Scanning electron microscopy (SEM) imaging principle is the spot-by-point scanning imaging of an electron beam on a sample surface. An electron beam with a certain energy is focused on an electron probe of a certain beam intensity under the action of an accelerating voltage and scanned on the surface of the sample. At the same time, interaction with the sample surface generates a physical signal that excites backscattered electron (BSE), X-ray, secondary electrons, and other imaging signals[1]. The detector collects the physical signal and converts it into an electrical signal and inputs it into the kinescope to modulate the brightness of the kinescope that is scanned synchronously with the incident electron beam. Combined with an X-ray energy dispersive spectrum analyzer

(spectrometer), the detector can reflect the surface morphology of the sample, Secondary electron images of structural composition and element distribution, backscattered electron images, X-ray images, etc. Image information is processed to obtain scanned electronic images representing the surface topography of samples [2]. Scanning electron microscopy has the characteristics such as large depth of field, large magnification range (generally 20 to 200,000 times), and its resolution can reach nanometer scale. The imaging has a three-dimensional, real sense, and easy identification. It is suitable for observing and analyzing heterogeneous compositions of heterogeneous materials[3].

The elements on the surface of the sample are excited to generate characteristic X-rays of each element under the irradiation of an electron beam with a certain energy. The energy of X-rays corresponding to each element has the following relationship with the X-ray wavelength[4].

$$E = hc / \lambda \quad (1)$$

E is the photon energy of the generated X-ray; h is the Planck constant; c is the light speed; λ is the X-ray wavelength.

According to formula (1), it can be seen that the ray corresponding
element can be found by determining the photon energy in the X-ray. An X-ray energy dispersive spectrum analyzer (EDS) can finish the job. The spectrometer is generally composed of four parts: a control system, a signal detection system, a signal conversion and storage system, and a result display system. With the aid of multi-channel pulse analyzers, the spectrometer can perform simultaneous quantitative and qualitative analysis of different elements in parallel, ie simultaneously. Therefore, the current scientific research usually combines scanning electron microscopy (SEM) and energy spectrometry, which has the advantages of high analysis speed, precise micro-area fixed-point analysis, and line and area scanning analysis. In the research of this subject, it is necessary to accurately identify the phase represented by each pixel at a certain section in the cement sample, and the morphology of each phase is not fixed, so it can only be identified based on the elemental composition. Therefore, backscattered electron images and X-ray images are valuable for the study of this project[5].

The secondary electron image and the backscattered electron image in the scanning electron microscope reflect the morphology of the sample, but the secondary electron image has a rich three-dimensional view, and has the advantages of high resolution, no obvious shadow effect, large depth of field, and strong stereoscopic effect, which is particularly suitable for observation of the morphology of a sample with a rough sample surface or a fractured surface structure. The backscattered electron image requires the sample surface to be sufficiently smooth and flat, because the brightness of the backscattered electron image of the smooth surface of the sample is proportional to the average atomic number of different phases in the plane, and the backscattered signal is stronger for the phase with the higher atomic number, at the same time, the brighter in the BSE image[6]. Therefore, the backscattered electron image is better applied to the study of the smooth surface of the cement sample after polishing, and the secondary electron image is more suitable for the observation of the microscopic appearance of the concrete sample in different parts of the sluice concrete structure in this project[7].

Therefore, the combination of scanning electron microscopy (SEM) and energy dispersive spectroscopy (EDS) can be used to characterize the morphological characteristics and changing rules of concrete microstructure in various parts of sluice concrete structures intuitively and comprehensively, analyze the main components and their relative contents, and then establish the correspondence between the microstructure characteristics and macroscopic properties of concrete materials[8].

3. Analysis of test results

3.1. floor

The left surface of the bottom plate of the sample is slightly smooth and dark gray; the right surface of the sample is rough, and the color is darker than the left and is variegated. The sandpaper left the

surface without powder particles falling, and the right surface was powdered particles falling. The initial observation of the sample shows that the left side is rock and the right side is mortar.

The SEM image of the sample on the bottom plate is shown in figure 1. In the figure, the yellow arrow marks the area where the microscopic structure is distributed in blocks and has sharp corners; the blue arrow marks the area where the microstructure is very loosely cemented with small particles protruding. The boundaries between the yellow and blue areas are clear and distinct. The blue area was initially determined as a mortar, and the yellow area was a rock. The area near the middle dividing line was an interface overgrowth region. Its thickness was longer than that of the middle pier and was about 40um,and no obvious cracks and acicular crystals were generated in the SEM observation area.

The Mg elemental surface analysis is shown in figure 2. Mg element enrichment appears on the right side of the observation area, and the content of Mg element on the left side is less. The surface scan image of the Mg element is in good agreement with figure 1 and figure 4 . In areas where a large amount of Mg elements are accumulated, the Si element is also enriched. It is shown that the rocky region of figure 1 is mainly composed of Mg elements.

From figure 3, it can be seen that the Al elemental surface analysis shows that the Al element in figure 1 is judged to have a small amount of aggregates in the area of mortar and rock, with no obvious distinction. From figure 4, the elemental surface analysis of Si shows that the pattern is consistent with the pattern presented in figure 2, mainly on the right side of the sample. However, the effect matching with figure 2 is general. Since the surface of the sample is not smooth enough, some voids appear in the surface distribution image of the Si element, which cannot be completely matched with figure 2. However, the observations in figure 1 are basically verified. The yellow area is a rock area (rocky areas are mostly silicate minerals) and the blue area is a mortar area.

From figure 5, the elemental plane analysis of Ca shows that in the BSE image of the middle-pier sample, it was judged that there was an enrichment phenomenon in the left blue area of the mortar. The Ca element represents the presence of cement. There is also a small amount of Ca element distribution in the right area. Therefore, the observation result of figure 1 is verified, the blue area is mainly a mortar area, the yellow area is a rock area, and the rock area contains a small amount of Ca element. From figure 6, the Fe element surface analysis shows that there is no obvious regularity in the distribution of Fe throughout the observed area.

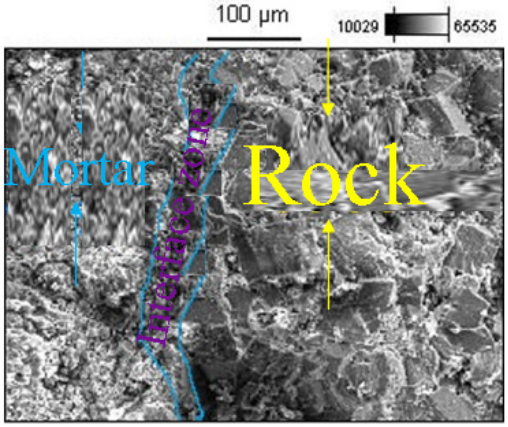

Figure 1 250x SEM image of bottom plate sample

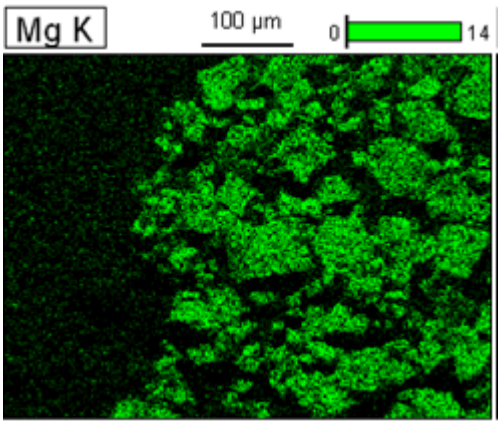

Figure 2 Mg element surface scan distribution map

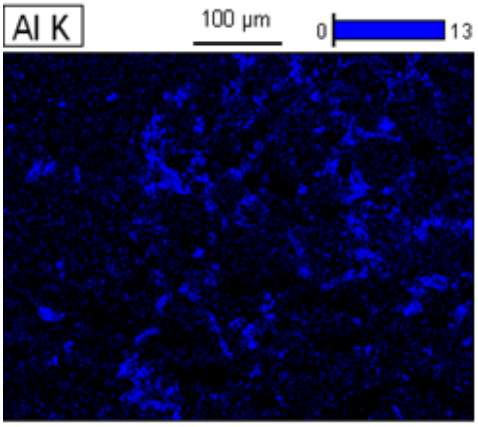

Figure 3 Al element surface scan distribution of floor sample

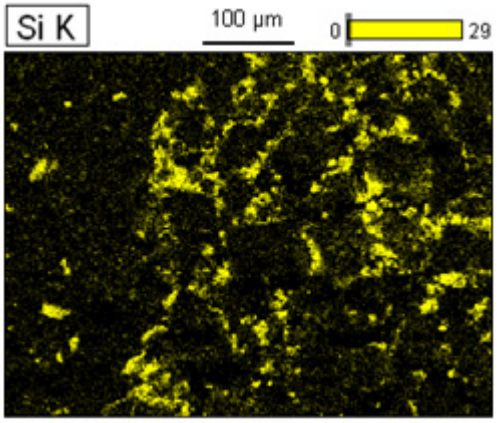

Figure 4 Si plate surface scan distribution map

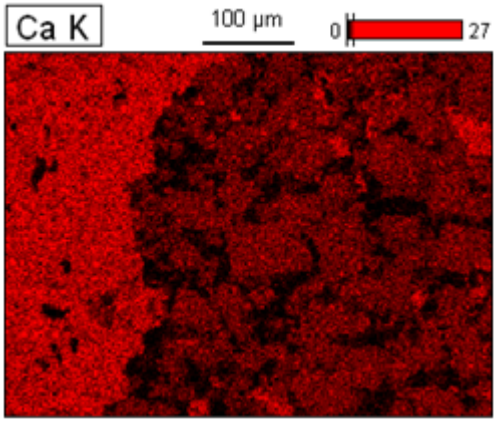

Figure 5 Floor element sample distribution map of Ca element

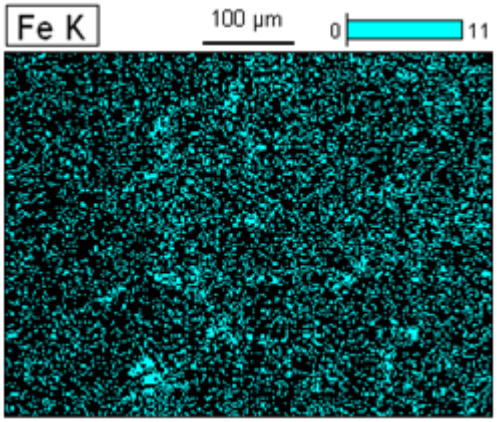

Figure 6 Surface scan distribution of Fe element on floor

At the 1 point of the baseplate sample SEM image, the distribution elements are mainly Si element, Al element, and O element; at the two points of the baseplate sample SEM image, the elements with the most distributed elements are Ca element and O element. Based on the above elemental analysis, it can be assumed that the 1 point is rock and the 2 point is mortar. Magnifications at the 1 point and the 2 point were respectively 500 and 1000 times, and btaining SEM images, showed that the prediction was correct and the surface was relatively smooth at the 1 point; the microstructure of the slurry at the 2 point was very loose. The interface transition zone thickness is approximately 40um. There were no obvious cracks and needle-like crystals in the sample observation area.

Table 1 Sample analysis of floor scans (%)

	C	O	Mg	Al	Si	S	Ca	Fe
Pt1	16.73	48.63		6.64	28.00			
Pt2	12.53	50.99	1.08	6.88	5.40		23.12	

3.2. Covering

The lower surface of the sample was covered with a block, slightly smooth, and dark in color; the upper surface of the sample was rough, and the color was darker than the left and was variegated. The sandpaper was ground and no powder particles were dropped on the surface, and powdered particles were dropped on the polished surface. The initial observation of the sample shows that the lower side is a rock and the upper side is a mortar.

According to the SEM image of the sample of the covered area, the surface of the sample is uneven and uneven. The thickness of the interfacial transition zone is about 30 um, and there are no obvious cracks and acicular crystals in the SEM observation area.

From the Mg elemental surface analysis chart, it can be seen that the Mg element enrichment phenomenon appears in the yellow region of the SEM observation area, and the distribution of Mg elements in other regions is less. In areas where a large amount of Mg elements are accumulated, the distribution of Ca elements is very small and almost absent. Therefore, it is indicated that the rock area contains mainly Mg elements.

The surface scan of the Al element shows that the distribution of the Al element in the observed area of the overlay sample is consistent with that of the Si element, accumulating in a large amount above the observation area of the sample. From the surface analysis chart of Ca element, Ca was found to be enriched in the blue area of the mortar in the covered sample, and was not distributed in the yellow area where the rock was judged. From the surface analysis of the Fe element, we can see that there is no obvious regularity in the distribution of Fe throughout the observed area.

At the No. 1 point of the SEM image of the covered sample, the distribution elements are mainly Ca, Si, and Mg; At the No. 2 point of the SEM image of the covered sample, the distribution elements are mainly Ca, and Si. Based on the above analysis of the elements, it can be speculated that the rock was at No. 1 spot and the mortar was at No. 2 spot. The thickness of the interface transition area is approximately 30um. There were no obvious cracks and needle-like crystals in the sample observation area.

3.3. Middle-Pier

The sample from middle-pier was selected for microscopic analysis with scanning electron microscope. The lower part of the sample is slightly smooth and dark gray; the upper part of the sample is rough, and the color is darker than the left part and is variegated. Grind the left surface with sandpaper and no powder particle falls down; grind the right surface with powder particles falling. According to preliminary observations, the lower part of the sample is rock and the upper part is mortar.

The thickness of the interfacial transition at the middle pier was about 20μm, and no obvious cracks and acicular crystals were found in the SEM observation area. From the surface analysis diagram of Mg element, Mg ion enrichment occurred above the SEM observation area, and Mg ion content was less in other areas, which indicates that the upper substance in the SEM observation region also contains relatively concentrated Mg and Fe elements. From the surface analysis of the Al element, it can be seen that Al in the BSE image of the middling sample was found to be enriched in the yellow area of the rock, with less distribution above the observation area. The Si element is also enriched in the yellow region where the Al element is heavily concentrated, while there is no Ca element in the yellow region, and the boundary line is completely clear. According to the consequence of observation, rock is in the yellow zone and mortar is in the blue one. The main metal element of the rock is Al.

At the 1 point of the back scattering image of the middle pier sample, the distribution elements are mainly Si, Al, and O; at the 2 point of the back scattering image of the middle pier sample, the distribution elements are mainly Ca and O; Based the analysis results above, it can be assumed that rock is at the 1 point and mortar is at the 2 point. The thickness of the interfacial transition area is approximately 20um. There are no obvious cracks and needle-like crystals in the sample observation area.

Table 2 Results of point sweep analysis of middle pier samples (%)

	C	O	Mg	Al	Si	S	Ca	Fe
Pt1		50.50		2.81	46.69			
Pt2	7.45	51.22	1.01	0.83	9.62	0.33	29.54	
Pt3		27.71			0.62			71.66

4. Conclusion

According to the results of the microscopic analysis, the main metal element in the rock area at the middle pier is Al. The thickness of the interface area of the middle pier is about 20 μm. The microstructure of the mortar area is dense, and there are no obvious cracks and acicular crystals in the sample observation area; The main metal element in the rock area at the bottom plate is Mg. The thickness of the interface area of the bottom plate is about 40um, the microstructure of the mortar area is loose, and there are no obvious cracks and needle-like crystals in the observed area of the sample; The main metal element in the covered rock area is Mg. The thickness of the interfacial area of the overlay is about 30 μm. The microstructure of the mortar area is dense, and there are no obvious cracks and needle-like crystals in the observed area of the sample. According to the microscopic test results of the sample, the greater the interface thickness of the microstructure of the concrete is, the lower the compressive strength of the component is. The widths of the interface area of the middle pier, the bottom panel and the overlay are approximately 20 μm, 40 μm, and 30 μm respectively; the corresponding compressive strength is the largest in the middle pier, followed by the second floor, and that of the floor area is the lowest. Studies have shown that sulfate corrosion is an important factor of aging of concrete structure, and ettringite, gypsum and other crystals produced in the interface transition zone of concrete are important causes of concrete damage. No crystals such as needle crystals and columnar crystals were found in the microscopic test of the concrete structure. The results of the compressive strength test proved that the concrete samples had higher compressive strength, indicating that the durability of concrete after running for more than 50 years was relatively good.

Acknowledgments

This work was supported by National Key R&D Program of China (2016YFC0401602)，National Natural Science Foundation(41671504)and Fundamental Research Funds of Nanjing Hydraulic Research Institute (Y717009).

References

[1] Zhu Bo-fang. On the expected life span of concrete dams and the possibility of endlessly long life of solid concrete dams[J]. Journal of Hydraulic Engineering, 2012,43 (1):1-9.
[2] Fan Yuncang, Cao Xingguo, Chen Huairong. Protection and Repair of Reinforced Bar Corrosion in Concrete[M]. Beijing: China Railway Press, 2001.
[3] Wang Haiyong, Zhou Chunlei, Bai Yun. Research on reasons and control measures about reinforced concrete damaged by corrosion[J]. China Building Materials Science & Technology, 2010，4(4)：32-34.
[4] Li Weiwen, Huo Yuan, Jin Zuguang. Research on the Durability of Buildings under the Action of Multi-factors[J]. Low Temperature Architecture Technology, 2009，11(11)：56.
[5] Gu Feng. Rebar Corrosion and Its Effect on Bridge Structural Performance[J]. Science & Technology Information, 2009，9(27)：266.
[6] Wu Fangguo, Wang Jifang. EXPERIMENTAL STUDY ON OUTER TEMPERATURE AND MOISTURE INFLUENCE ON REINFORCING STEEL CORROSION UNDER CHLORION CONTENT[J]. China Science and Technology Information, 2008，5(9)：71-72.
[7] Jin Dan. Study on Microporous Structure of Cement-based Materials by NMR[D]. Nanjing: Hohai University, 2016.
[8] She Anming. State Evolution of Water in Cement Paste and Its Relationship with Paste Hydration Process and Microstructure[D] Shanghai: Tongji University, 2010,11.